Photopyroelectric thin-film instrumentation and impulse-response detection. Part II: Methodology

Joan F. Power and Andreas Mandelis

Photoacoustic and Photothermal Sciences Laboratory, Department of Mechanical Engineering, University of Toronto, Toronto, Ontario M5S 1A4, Canada

(Received 7 May 1987; accepted for publication 21 July 1987)

Frequency-modulation time-delay spectrometry (FM-TDS) has been implemented in photopyroelectric measurements of thermal diffusivity, on a series of well-characterized samples. The strategy of FM-TDS is sample excitation by a fast linear frequency sweep, whose autocorrelation function is mathematically equivalent to a Dirac delta function. The method permits the fast recovery of high-quality frequency and impulse-response information. Impulse responses recovered in the time-delay domain showed good agreement with a Green's function model of transient heat conduction. The present work demonstrates that the FM-TDS measurement strategy yields photothermal information equivalent to that obtainable from a pulsed laser system, with much lower excitation power.

INTRODUCTION

Photopyroelectric methodologies have emerged in recent years as new and powerful techniques for the measurement of both thermal and optical absorption properties of solids.[1–4] Because of its nondestructive character, sensitivity, and relative experimental simplicity, photopyroelectric spectroscopy (P^2ES)[1–7] is capable of providing thermo-optic information on a variety of geometric structures which are accessed with difficulty using conventional techniques. Of special interest to nondestructive (materials) evaluation is the measurement of thermal diffusivity or material thickness information on very thin samples. Here, photopyroelectric methods have demonstrated a history of success on materials ranging from thin metallic films to polymer laminates[5–7] and other composite structures.

The strategy of photopyroelectric methods uses light absorption by the sample to generate thermal waves in the material via localized heating. Laser excitation, in particular, enables the generation of a spatially well-defined thermal source in the sample. The signal generation mechanism in P^2ES is essentially typical of photoacoustic and photothermal methods, in general, with the important difference that the P^2ES measurement strategy involves detection via a thin-film pyroelectric effect device in physical contact with the back surface of the (thin) sample. The pyroelectric element functions as a calorimeter, giving rise to an electrical signal in response to a change in the average temperature of the element. In contrast with other photothermal and photoacoustic methods, which usually measure thermal signals arising from energy deposited within a thermal diffusion length of the sample surface,[8] photopyroelectric detection relies on the measurement of energy transmitted through the material. Furthermore, pyroelectric thin films function as direct detectors of temperature changes in materials, in contrast with related photothermal and photoacoustic methods which rely on secondary mechanisms of detection such as sound wave generation,[8] or beam deflection by refractive index changes in the sample or a (usually fluid) coupled detection medium.[9,10] The fast rise-time capabilities of thin-film pyroelectric effect detectors such as polyvinylidene difluoride (PVDF or PVF_2) make them ideal candidates for impulse response measurements.[1,2,5]

The acquisition of thermal wave information in P^2ES may be achieved via several measurement approaches, including (a) single-frequency harmonic excitation and detection of thermal wave phenomena using sinusoidally modulated cw irradiation of the sample,[7] (b) pulsed excitation with observation of transient signals,[5,6] or (c) wide-bandwidth (modulated cw) signal generation[10–13] with simultaneous excitation and detection of the entire thermal wave-frequency-response spectrum of the sample. Classical P^2ES techniques use single-frequency cw harmonic excitation and detection in which the sample's frequency response is recorded on a point-by-point basis, using lock-in amplification. The disadvantages of the method include long-time scales required for signal measurements, as well as the general disadvantage of interpreting frequency-domain information, which is usually not directly visualized in terms of the propagation times of thermal signals through the sample material. The method retains the advantage of using low-powered, stable cw excitation sources. The situation may be contrasted with pulsed excitation methods which have exhibited considerable success in P^2ES.[5,6] An important advantage of transient excitation is that it yields impulse response information which is directly interpretable in terms of the transit times of thermal signals transmitted by the sample. Impulse-response information for well-defined material layers is directly interpretable in terms of layer thickness or thermal diffusivity via Green's function models.[6,11,14–16] The disadvantages of pulsed techniques include high peak power requirements for sample excitation, with a corresponding low damage threshold for many delicate materials, including semiconductors and photosensitive thin films.

A more recent method of signal recovery involves the use of the broadband-modulated cw excitation with simultaneous detection of all components of the photothermal system's frequency response. Fast Fourier transform[10–13] and correlation analysis techniques[17] enable the recovery of both high-resolution-frequency-response and impulse-response

 0034-6748/87/112024-09$01.30

information. Because of the FFT character of the data analysis, the entire frequency spectrum of the photothermal system is captured and analyzed at high speed. The time resolution of the impulse-response information made available by the method is limited only by the bandwidth and the transfer function of the detector of the excitation waveform. Consequently, broadband cw excitation methods yield the equivalent of pulsed response while retaining the advantages of low excitation power, and the high source stability available from cw laser systems. The primary advantages are a dramatic increase in the damage threshold of the samples under study, a potentially improved signal-to-noise ratio (because of improved source stability and higher dynamic range of the response to certain forms of excitation), and a great increase in speed and data resolution.

Broadband cw excitation methods can generally induce (a) stochastic and (b) deterministic stationary signal generation.[17,18] The former class consists of random and pseudorandom excitation,[12,16,19] while the latter is typified by the more recently developed technique of frequency-modulation time-delay spectrometry[10–12,20–22] (FM-TDS). FM-TDS involves excitation of the photothermal system using a fast linear frequency sweep. The excitation sweep contains all of the frequencies which comprise the response band of the photothermal system, so that, like random and pseudorandom techniques, the autospectrum of the excitation wave train is flat. (Alternatively, in the time-delay domain, the wave train is mathematically equivalent to a Dirac delta function.) The performance of FM-TDS is superior to random and pseudorandom techniques with respect to dynamic range and the rejection of extraneous noise.[20–22] The application of FM-TDS was recently demonstrated, for the first time in photothermal detection, by Mandelis *et al.*,[10–12] and showed the same superior performance over pseudorandom techniques.

In this work, we report for the first time the extension of FM-TDS to thermal wave detection using the photopyroelectric effect. The methodology reported in this work has direct applications for thermal diffusivity and conductivity measurements on solid samples, and for the imaging of thin structures with spatial variations of thermal properties. The recovery of thermal diffusivity or layer thickness information is described by recourse to a Green's function model of transient heat conduction (this work, Part I), and applied to a series of well-characterized samples.

I. EXPERIMENTAL

A. Apparatus design and characterization

The design of our time-delay-domain photopyoelectric detection system is summarized in Fig. 1. The excitation source was a Coherent Innova 90 cw argon ion laser operating single line at 488 mm. The excitation power used in these experiments ranged from 100–200 mW depending on the sample thickness. The central excitation/detection component in the system was a HP 3562 fast Fourier transform analyzer equipped with an internal frequency synthesizer. The synthesizer was capable of generating fixed sine and random noise waveforms, as well as linear frequency sweeps,

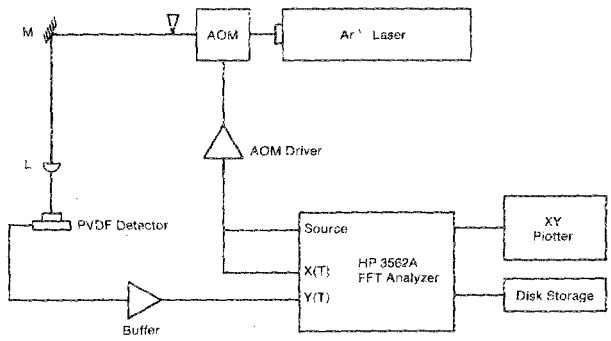

FIG. 1. FM time-delay photopyroelectric spectrometer apparatus. See text for details.

with modulation bandwidths up to 100 kHz. The sweep source was used to drive an acousto-optic modulator (Isomet 1201E) to modulate the intensity of the Ar^+ beam using a knife edge. The output of the acousto-optic modulator was optimized for modulation depth and minimum distortion by adjusting the peak-to-peak voltage applied to the driver circuit to a value of 400 mV. A reference beam was obtained by recording a fraction of the excitation signal with a beam splitter (BS) and a photodiode (PD). The photodiode input was used as a measure of the excitation waveform $x(t)$. In some experiments, the output of the HP 3562A internal synthesizer was used to supply the $x(t)$ waveform. The main excitation beam was directed through a microscope objective lens (magnification: 32×) (L1) to simulate a point source, and focused onto the surface of a thin-film pyroelectric detector (PED) or a sample. The detector consisted of a 28-μm film of polyvinylidene difluoride (PVDF) (Penwalt Corporation "KYNAR" piezo film)[23] supported by a stainless-steel backing. The detector was enclosed in an assembly supplied by Inficon to provide electrical contact and to ensure shielding from electromagnetic rf interference. Thermal contact between the sample and the detector was optimized by using a thin layer of thermally conducting grease (No. 120-8, Wakefield). The output of the detector was fed to a high-impedance buffer preamplifier (Comlinear, CLC-B-600, 3-pF parallel 3-MΩ input impedance; 600-MHz bandwidth), and applied to the $y(t)$ system input of the HP 3562A FFT analyzer. The recovery of all frequency and time-delay-domain functions was achieved via the analyzer computations.

B. Nature of recovered FM-TDS P²E signals

In order to successfully implement FM-TDS for the measurement of linear system responses, certain criteria must be met with respect to the frequency spans of input and output spectral density functions. These criteria have been discussed in past work[10] but are briefly outlined here. Any photothermal system may be modeled as a general linear system or "black box" (Fig. 2) with impulse response $h(\tau)$, input wave train $x(t)$ and output response $y(t)$. In experiments involving broadband excitation, the power spectrum of the input, $G_{xx}(f)$, is assumed to be flat, or "white," relative to the power spectrum of the response, $G_{yy}(f)$.[10,13,18] In FM-TDS as in random noise excitation methods,[10,17] the fre-

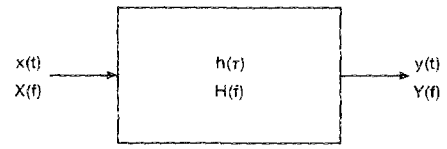

FIG. 2. Generalized "black-box" representation of frequency response $H(f)$ for a photothermal system.

quency response is recovered from a cross-spectral measurement as

$$H(f) = G_{xy}(f)/G_{xx}(f), \tag{1}$$

so that if $G_{xx}(f) = 1$, then $H(f) = G_{xy}(f)$. Equivalently, a flat input power spectrum yields an autocorrelation function $R_{xx}(\tau)$ which is mathematically equivalent to a Dirac delta function, by inverse transformation to the time-delay domain:

$$R_{xy}(\tau) = R_{xx}(\tau)*h(\tau) = \delta(\tau)*h(\tau),$$

or

$$R_{xy}(\tau) = h(\tau). \tag{2}$$

In the case of FM-TDS where the excitation wave train is a linear frequency sweep (Fig. 3), the criterion for flatness of the input autospectrum, $G_{xx}(f)$, is met when the sweep time T is much longer than the longest time-delay component τ in the system response,[10,21,22] and when the product of the modulation bandwidth, Δf and T, is very large, well above the limit of the instrumental uncertainty principle:

$$(\Delta f)T \gg 1. \tag{3}$$

Typical excitation and response signals for a 28-μm PVDF pyroelectric thin-film detector in an FM-TDS experiment are shown in Fig. 3. Swept waves were generated in the HP 3562A internal source with frequency spans ranging from 0–25 Hz (for thermally thick samples with slow time-delay-domain response) to up to 0–25 kHz, (for thermally thin samples, with rise times approaching that of the pyroelectric film itself). The swept waves generated within the HP 3562A were used to drive the acousto-optic modulator. Measurements carried out with the HP 3562A FFT analyzer were made in the linear resolution mode. In that mode the sweep time was related to the frequency span by the relationship[24]:

$$T(\mathrm{s}) = 800/\Delta f(\mathrm{Hz}), \tag{4}$$

where the frequency span Δf is the modulation bandwidth of the carrier ($\Delta f = f_2 - f_1$) with $f_1 = 0$, and f_2 the maximum frequency in the sweep. The product $(\Delta f)T$ approaches 10^3, which ensures flatness of the excitation autospectrum, $G_{xx}(f)$.[20–22] In all cases, the sweep was unidirectional from f_1 to f_2, and the resolution of the input data was 2048 points/sweep, with the sampling rate set above the aliasing frequency at $2.56 f_2$.

In measurements made using our photopyroelectric system we have found, in practice, ringing effects in the recovered frequency responses. The origin of these artifacts was traced to the power spectrum of the modulator output, despite efforts expended at adjustment of the modulation depth for minimum distortion. As discussed in detail in Part III of this work, the effect of these frequency-domain artifacts appears to be unimportant in the time-delay regime yielding thermal transit time information. Impulse-response information recovered by inverse Fourier transformation of frequency response data containing the distortions was shown to yield time-delay-domain signals congruent with $h(t)$ data obtained by random noise measurements from which these artifacts were absent.[25] It was possible to make undistorted measurements of the frequency response by lowering the drive voltage on the modulator to minimize nonlinearities in the output. The magnitude and phase response of the PVDF detector signals, recovered by FM-TDS are shown to compare favorably with standard $H(f)$ data obtained by lock-in measurements and very slow sine sweeps (Figs. 4 and 5). The TDS data were recorded in a fraction of the time required for the lock-in measurement, and at far greater resolution (2048 data pts/sweep). The latter type of measurement, in turn, limits the resolution of any impulse-response information that would be available from inverse transformation of frequency-domain data acquired via lock-in detection.

From the data of Figs. 4 and 5, it can be seen that the frequency response obtained from the pyroelectric thin film is weighed towards the lowest-frequency components. The features of the film response underline a general feature encountered in P^2E signal analysis typical of the diffusive nature of thermal waves: The strong response at low frequencies contains little information related to the transit time of thermal signals transmitted through the film. As shown in the impulse responses of Fig. 6 for the PVDF thin film detector, the thermal transit time information is observed at short

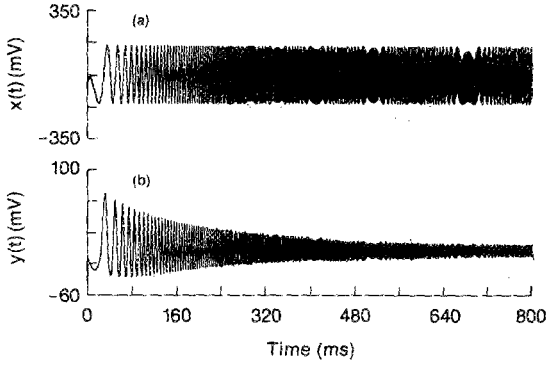

FIG. 3. FM time-delay swept wave excitation and response signals (a) input wave train $x(t)$; (b) PVDF thin-film detector response $y(t)$. $\Delta f = 0$–1 kHz. Sweep rate: 1.25 kHz/s.

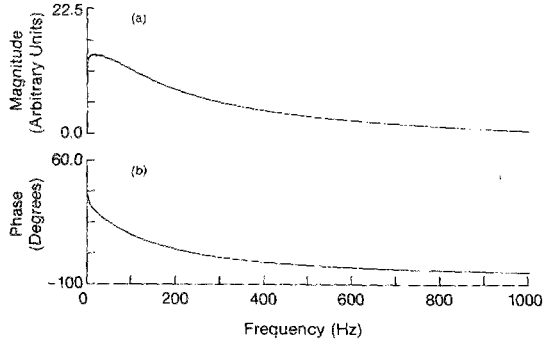

FIG. 4. Magnitude (a) and phase (b) of the frequency response (transfer function) of 28-μm PVDF pyroelectric thin-film detector. Measurements were made with point-by-point sinusoidal excitation and are equivalent to results obtained with lock-in detection. Sweep rate: 2.74 Hz/s.

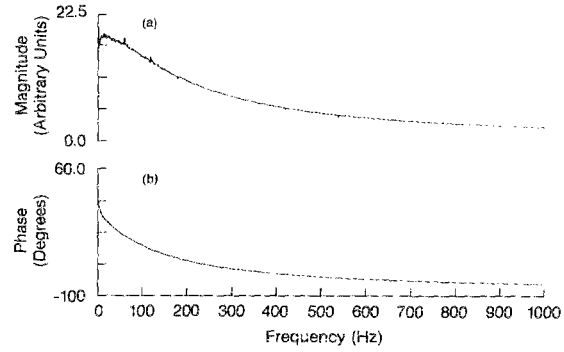

FIG. 5. FM time-delay measurements of frequency response for thin-film (28-μm) PVDF detector. Magnitude and phase; Δf = 0–1 kHz; Sweep time; 800 ms. Measurement is the result of 300 averages.

time delays ($\tau < 2$ ms) which correspond to high frequencies under Fourier transformation. The high-frequency information is of low magnitude relative to the lower frequencies.

As already discussed, the success of the FM-TDS measurement depends on the approximation of the input autocorrelation function to a Dirac delta function in the time-delay domain, or alternatively, on the flatness of the input autospectrum, $G_{xx}(f)$. These relationships are illustrated in Fig. 7. A comparison of $G_{xx}(f)$ and $G_{yy}(f)$ recorded for the PVDF detector [Figs. 7(a) and 7(b)] indicates that $G_{xx}(f)$ is nearly flat over the frequency range of 0–1 kHz. The oscillatory components at the edge of the span arise from the finite sweep time used in these experiments, which reduces the approximation of $R_{xx}(\tau)$ to a time delta function.[21] The output power spectrum $G_{yy}(f)$ appears to be of very low magnitude at the top of the frequency span.

This situation should be interpreted cautiously, however, because in the frequency domain the output amplitude $y(f)$ is the square root of the power and may be significantly greater than is indicated by a casual inspection of $G_{yy}(f)$. While the condition $G_{xx}(f) \simeq 1$ appears to be satisfied at Δf = 0–1 kHz [Fig. 7(a)], the corresponding impulse response recorded at this frequency span [Fig. 6(a)] shows a poor resolution at early time delays. The 0–1 kHz frequency span is therefore insufficient to resolve the rise time of the detector element, since the much weaker, high-frequency components associated with these early time delays lie outside the modulation bandwidth of the sweep. This point is also illustrated in Figs. 7(c) and 7(d) which compare the input and output autocorrelation function $R_{xx}(\tau)$ and $R_{yy}(\tau)$, for the PVDF detector at Δf = 0–5 kHz. While $R_{xx}(\tau)$ approximates to a delta function to within the time-delay linewidth defined by the modulation bandwidth of the sweep, the width of $R_{xx}(\tau)$ is not negligible compared with $R_{yy}(\tau)$. Increasing the modulation bandwidth of the sweep to Δf = 0–25 kHz enables the resolution of the detector rise-time information in the impulse respone [Fig. 6(b)]. The improved approximation of $R_{xx}(\tau)$ to a delta function relative to $R_{yy}(\tau)$ is indicated in Figs. 7(e) and 7(f).

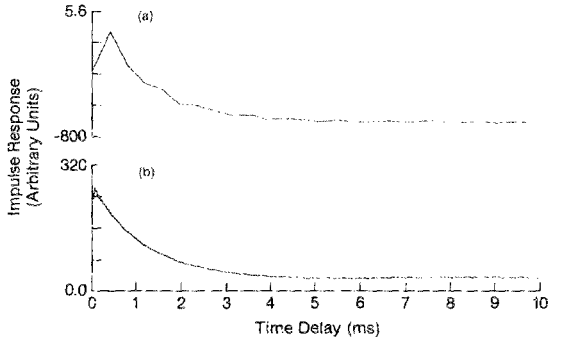

FIG. 6. Impulse response information recovered for thin-film PVDF detector with different modulation bandwidths. (a) Δf = 0–1 kHz (b) Δf = 0–25 kHz. Each figure was the result of 100 averages. Peak delay information as follows: (a) $\tau_d = 390.6$ μs; $\Delta\tau_d$, 976.5 μs (b) $\tau_d = 62.5$ μs, $\Delta\tau_d$ = 843.75 μs.

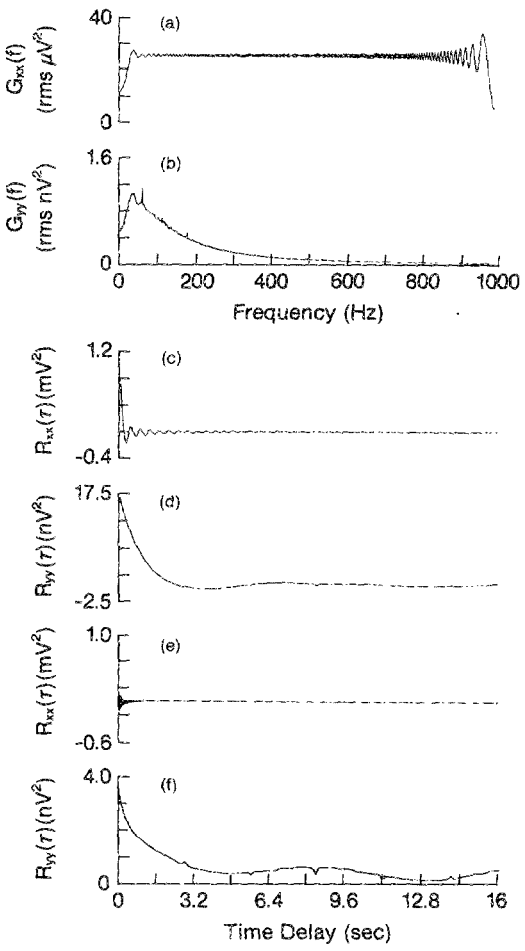

FIG. 7. Power spectra and autocorrelation functions for PVDF thin-film detector. (a) $G_{xx}(f)$ and (b)$G_{yy}(f)$ recorded with Δf = 0–1 kHz, (c) $R_{xx}(\tau)$ and (d) $R_{yy}(\tau)$ recorded with Δf = 0–5 kHz, (e)$R_{xx}(\tau)$ and (f) $R_{yy}(\tau)$ recorded with Δf = 0–25 kHz.

For samples in contact with the pyroelectric film, the frequency response of the sample/pyroelectric system is shifted to lower frequencies corresponding to a range of increasing time delays. This shift is due to the finite propagation time to thermal wave signals through the sample material, which delays the arrival of temperature changes at the PVDF detector surface. For thick samples, the shift may be quite pronounced (Fig. 8), with the result that lower frequency spans are required to resolve the impulse response information. A consequence of this condition, in the present system, is that the sweep time decreases to maintain constant

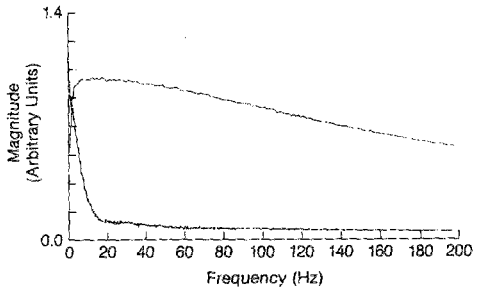

FIG. 8. Comparative frequency response magnitudes recorded for PVDF thin-film detector (upper curve) and 400-μm quartz sample (lower curve). Both measurements were made with slow sine sweeps (sweep rate <3 Hz/s).

(2048 point) data resolution [Eq. (4)]. Slower sweep times also prevent the possibility of nonlinear photothermal responses which occur when the sweep time T is less than the longest time-delay components in the photothermal system. In such cases, nonequilibrium system responses could occur, in which no proper Fourier transforms would exist, as the Fourier coefficients in the response would be functions of time or frequency.

A further indication of the quality of an FM-TDS measurement is the degree of agreement between $h(\tau)$ and the cross-correlation function $R_{xy}(\tau)$ in accordance with Eq. (2). Figure 9 makes this comparison for the pyroelectric thin-film detector and for a 400-μm glass sample, coated with a thin layer of ink acting as a surface thermal source. Agreement between the two time-delay-domain functions is excellent with respect to peak-delay information, indicating the success of the FM-TDS measurement strategy. The peak widths of the cross-correlation functions, however, are consistently narrower than the corresponding impulse-response peaks. This feature has been attributed to nonuniformities in the input power spectrum $G_{xx}(f)$ at the edges of the frequency span [Fig. 7(a) and Part III, this work].

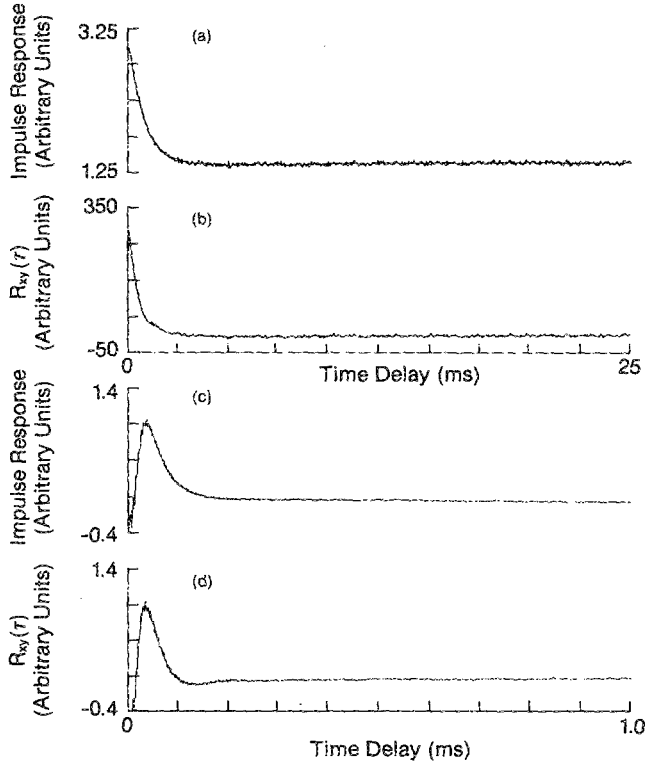

FIG. 9. Impulse response $h(\tau)$ and cross-correlation functions $R_{xy}(\tau)$ compared for (a) and (b) thin-film PVDF with $\Delta f = 0$–25 kHz; (c) and (d) 400-μm quartz sample and $\Delta f = 0$–200 Hz. $N = 300$ averages. Time-delay information was: PVDF (a) $h(\tau)$, $\tau_d = 62.5\,\mu$s, $\Delta\tau_d = 844\,\mu$s; (b) $R_{xy}(\tau)$, $\tau_d = 62.5\ \mu$s, $\Delta\tau_d = 470\ \mu$s; 400-μm quartz (c) $h(\tau)$, $\tau_d = 35.16$ ms, $\Delta\tau_d = 29.5$ ms; and (d) $R_{xy}(\tau)$, $\tau_d = 35.16$ ms, $\Delta\tau_d = 25.9$ ms.

C. Thermal diffusivity and material thickness measurements on thin solid samples

In order to characterize the response of our instrument and demonstrate its capabilities for thermal diffusivity measurements, we have recorded and theoretically modeled the responses of a series of well-characterized samples. These samples consisted of a series of quartz microscope slides and cover slips of varying thickness. Each series of samples was prepared from a single slide, cut in many smaller pieces, to ensure material uniformity. The pieces were etched in 50% HF/50% H_2O to the desired thickness. The front surfaces of these samples were coated with a thin layer of water soluble ink, which served as a blackbody layer. The thinness of the ink layer and its large absorption coefficient ensured that the laser radiation absorbed at the sample surface acted as an ideal plane heat source.

The impulse responses of these samples may be readily predicted from a Green's function model of transient heat conduction in a four-layer system. In Part I of this work, we presented a time-domain theory of photopyroelectric signal generation which accounts for the finite thickness of the detector element and the thermal properties of the backing. This theory is readily adaptable to the present results in which the thickness of the samples is large relative to the film thickness. The advantage of the theory is ease of interpretation and extraction of thermal transit time information from the P^2E response.

The current response for the pyroelectric detector element under load has the form[23,26]

$$V(t) = K\frac{\partial\langle T_d(x,t)\rangle}{\partial t}, \tag{5}$$

where $\langle T_d(x,t)\rangle$ is the spatially averaged temperature profile in the film, $V(t)$ is the voltage recorded at the output of the buffer preamplifier, and K is a constant which incorporates the electrical properties of the pyroelectric film.

The theory of Part I, interpreted for thermally thick samples, gives a pyroelectric response of the form

$$V(t) = \frac{KA}{t^{3/2}}\sum_{n=0}^{\infty}(-1)^n\gamma^n \times\left(\tau_{1n}^{1/2}e^{-\tau_{1n}/4t} - 2\tau_{2n}^{1/2}e^{-\tau_{2n}/4t} + \tau_{3n}^{1/2}e^{-\tau_{3n}/4t}\right), \tag{6}$$

where

$$\tau_{1n}^{1/2} = \frac{2nd}{\alpha_3^{1/2}} + \frac{l}{\alpha_2^{1/2}},$$

$$\tau_{2n}^{1/2} = \frac{(2n+1)d}{\alpha_3^{1/2}} + \frac{l}{\alpha_2^{1/2}},$$

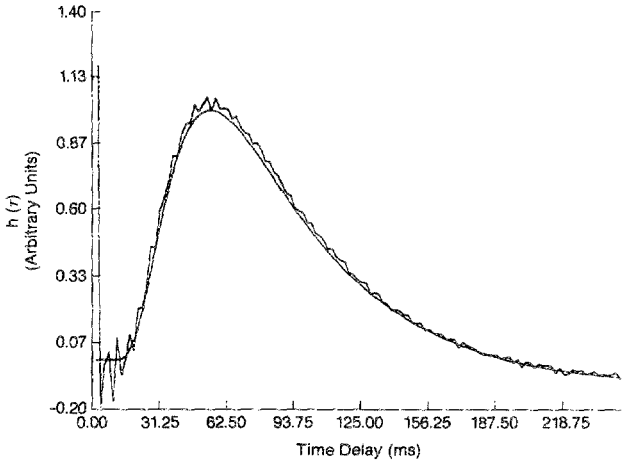

FIG. 10. Theoretical and experimental impulse-response profiles obtained for a 500-μm quartz sample.

$$\tau_{3n}^{1/2} = \frac{2(n+1)d}{\alpha_3^{1/2}} + \frac{l}{\alpha_2^{1/2}}.$$

The factor A is a constant which incorporates the static thermal properties of the sample/pyroelectric system:

$$A = -2(\alpha_3\alpha_2)^{1/2}/\alpha_2(b_{32}+1)4\sqrt{\pi}. \quad (7)$$

The subscripts 3 and 2 refer to the pyroelectric film and sample, respectively. Here, α_i is the thermal diffusivity of material (i). The coupling coefficients b_{ij} are defined as $b_{ij} = k_i\alpha_j^{1/2}/k_j\alpha_i^{1/2}$, where k_i is thermal conductivity. The parameter $\gamma = (b_{32}-1)/(b_{32}+1)$, and l,d refer to the thickness of the sample and film, respectively. Other assumptions of Eq. (6) are that there are large thermal mismatches at the sample/gas and film/backing interfaces: that is, $b_{12} \ll 1$ and $b_{43} \gg 1$.[27]

In this work, we have compared the results predicted by this model with our experimental impulse responses. Because the absolute intensity of the recovered signals is a function of instrumental factors such as irradiation power, amplifier gain, and excitation geometry, we have normalized the impulse responses to give $V(t) = 1$ at the peak of the time-delay response. Figure 10 shows the comparison between experiment and theory for a 500-μm sample of quartz. The impulse response profile was fitted assuming $\alpha_2 = 4.0\times10^{-7}$ m^2/s for quartz, which shows excellent agreement with literature values: $\alpha_2 = 4.0\times10^{-7}$ m^2/s (Ref. 28) and $\alpha_2 = 4.4\times10^{-7}$ m^2/s (Ref. 8). The value of the parameter γ which gave the best fit to experiment was $\gamma = 0.7$. From this parameter, it was possible to calculate the thermal conductivity for the sample as $k_2 = 2.2$ W/m K.

Agreement between theory and experiment is excellent in the time-delay domain from 0–1 s. The theoretical expression of Eq. (6) required approximately five terms for convergence. The poor agreement at early times is due to light leakage through the sample blackbody layer onto the surface of the film, which causes simultaneous excitation of the film response. The effect is generally more pronounced for thick samples with long time delays, since their peak intensities are weak relative to the early signals (Part I). Samples with earlier peak delays are generally less susceptible to this phenomenon because the signal intensity is much greater with the thinner samples.

The response of an entire set of samples is summarized in Fig. 11. For the series of quartz slides, plots were made of the time delay τ_d and peak width $\Delta\tau_d$ (as defined in Part I) versus the square of the sample thickness. The plots shown in Fig. 11 indicate excellent agreement between theory and experiment with respect to both parameters over the full range of samples studied. It is of further interest to note that the relationship between τ_d and l^2 predicted from theory is nearly linear ($R > 0.9999$ where R is the correlation coefficient) over a reasonable range of sample thicknesses. This relationship suggests that the photopyroelectric methodology described could be used for precision thickness measurements on thin layers of glasses, by preparing calibration curves of

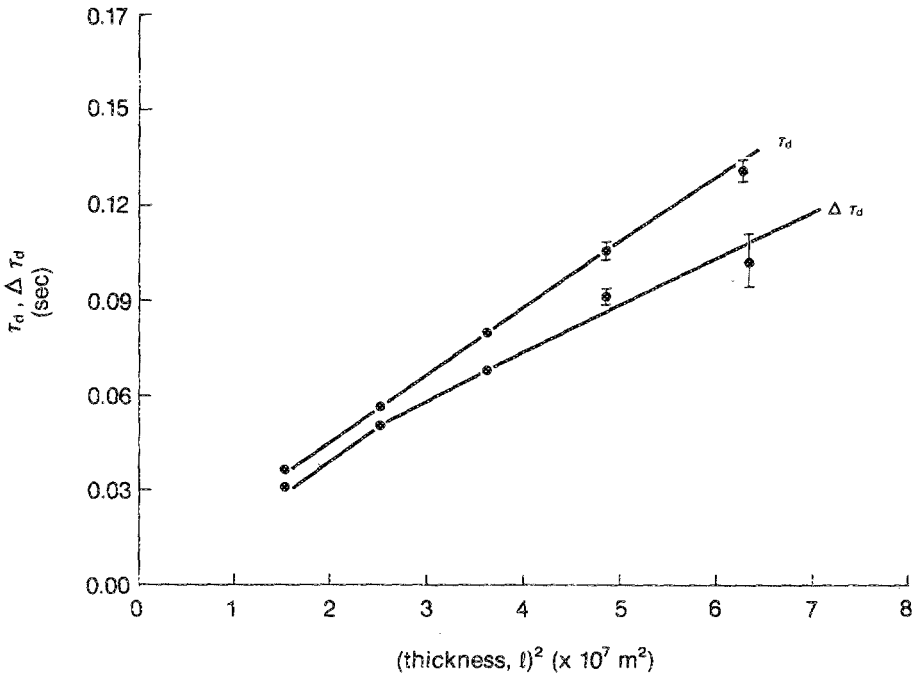

FIG. 11. Impulse-response parameters vs sample thickness for a series of well-characterized (quartz) samples. Solid lines represent theoretical responses.

TABLE I. Measured diffusivity values for selected materials.

Material	α_2(m^2/s) Experimental, This work	α_2(m^2/s) Literature values	Measurement conditions
Quartz, fused	4.0×10^{-7}	4.0×10^{-7} (Ref. 28)	l_{range}: 300 μm–1 mm
		4.4×10^{-7} (Ref.8)	τ_{range}: <1 s
Stainless steel	2.2×10^{-6}	3.5×10^{-6} (Ref. 29)	l_{range}: 390 μm–1 mm
			τ_{range}: <25 ms
Aluminum	38×10^{-6}	97.1×10^{-6} (Ref.29)	l_{range}: 500 μm–2 mm
		68×10^{-6} (cast) (Ref. 29)	τ_{range}: <10 ms

τ_d (or $\Delta\tau_d$) vs l^2 and thereby standardizing the photopyroelectric system.

We have also tested the methodology using metallic samples (aluminum, stainless steel) which were contacted to the pyroelectric (PVDF) detector using thermal compound. In the case of the metal samples, $b_{32}\ll1$, so that $\gamma=1$ in Eq. (6). The expression is valid provided $l^2/4\alpha_2\tau\gg d^2/4\alpha_3\tau$ (Part I). Thermal diffusivity measurements on these samples are reported in Table I which also reports the sample thickness and time-delay ranges for which the measurements were made. These conditions fall well within the approximations required by the model.

The results of Table I show a reasonable agreement between measured and literature values of α_2 for a wide range of different materials. The main factor controlling the agreement between theory and experiment for these results is the thermal contact resistance present at the sample/detector interface. Flatness of the sample surface promotes a good thermal contact with the detector film, while warpage or other surface deformities cause poor contact and an overestimated value of the measured thermal diffusivity. A residual contact resistance persisted in our sample/pyroelectric system, even when thermal coupling compound was used, and contributed appreciable errors in α_2 at time delays earlier than 5 ms.

II. DISCUSSION

Our Green's function model is a more complete version of an earlier theory derived by Yeack *et al.*[6] The two models are similar for the sample in contact with a semi-infinite pyroelectric detector. The earlier theory was well adapted to pyroelectric detection using solid-state detectors with relatively large thicknesses but it does not fully apply to the situation where the detector element is a thin film. In that theory, heat flow into the gas layer was assumed to be negligible, which is equivalent to setting the interfacial transport coefficient $b_{12}\sim0$. In Part I, we demonstrated that our four-layer model reduced to the Yeack *et al.* theory[6] when the thermal properties of the backing are identical to those of the film ($b_{43}=1$) and for the case when the film thickness d approaches infinity.

Like the earlier theory, our equations fit well for samples which are thermally thick, i.e., $l^2/4\alpha_2\tau\gg1$. In the present case, the condition $l^2/4\alpha_2\tau\gg d^2/4\alpha_3\tau$ (Part I) ensures a good approximation to Eq. (6). Also, in agreement with the earlier theory,[6] the peak delay is most strongly dominated by α_2 and l. Slight changes in γ result in an adjustment of α_2 by a factor of $<10\%$ to maintain optimum agreement between theory and experiment: that is, α_2 is relatively insensitive to γ so that a good estimate of α_2 is available from data fitted with a single thermal parameter.

The four-layer theory developed in Part I may also be interpreted for very thin samples in which $l^2/4\alpha_2\tau\ll d^2/4\alpha_3\tau$, but this condition is not pertinent to the present work because of the contact resistance effects that contribute with thin samples. For work with very thin layers, the samples should be directly deposited on the detector film surface using vacuum deposition, spin coating, or other techniques to ensure a good thermal contact.

The four-layer theory is well adapted to measurements on thick samples because the experimentally measured peak delay of $h(\tau)$ is due almost exclusively to diffusional processes, and the resistance effects are negligible. In the earlier work by Yeack *et al.*,[6] their theoretical model was extended to incorporate the effects of contact resistance between the sample and pyroelectric layers. The resulting expression explains the regime of contribution of contact resistance effects. Their expression for the Laplace transform of the temperature profile in the pyroelectric is, for a unit power source,

$$\overline{T}_d(x,s)=\frac{(-2/k_2)(\alpha_2/s)^{1/2}\exp\left[(l/\alpha_2^{1/2}-x/\alpha_3^{1/2})\sqrt{s}\right]}{(1-b_{32}+R_{th}k_3\sqrt{s}/\alpha_3^{1/2})-e^{2l\sqrt{s}/\alpha_2^{1/2}}\left[1+b_{32}+(R_{th}k_3/\alpha_3^{1/2})\sqrt{s}\right]}. \tag{8}$$

The denominator contains the factor $R_{th}k_3\sqrt{s}/\alpha_3^{1/2}$ which is due to the thermal contact resistance R_{th}. At early time delays, this term dominates because the Laplace domain variable $s\leftrightarrow2\pi j/\tau$. The Laplace transform of the temperature in the pyroelectric becomes

$$\bar{T}_d(x,s) = \frac{2(\alpha_2\alpha_3)^{1/2}\exp\left[(l/\alpha_2^{1/2} - x/\alpha_3^{1/2})\sqrt{s}\right]}{sR_{\text{th}}k_2k_3\left(1 - e^{-(2l/\alpha_2^{1/2})\sqrt{s}}\right)}, \tag{9}$$

which yields a time dependence of the form

$$T_d(x,t) = \frac{2(\alpha_2\alpha_3)^{1/2}}{R_{\text{th}}k_3k_2} \times \sum_{m=0}^{\infty} \text{erfc}\left[\left(\frac{x}{\alpha_3^{1/2}} + \frac{(2m-1)l}{\alpha_2^{1/2}}\right)\frac{1}{2t^{1/2}}\right]. \tag{10}$$

Alternatively, at longer time delays, s is small and the diffusional term in the denominator dominates:

$$\bar{T}_d(x,s) = \left(\frac{-2\alpha_2^{1/2}}{k_2 s^{1/2}}\right)\frac{\exp\left[(l/\alpha_2^{1/2} - x/\alpha_3^{1/2})\sqrt{s}\right]}{(1-b_{32}) - (1+b_{32})e^{-(2l/\alpha_2^{1/2})\sqrt{s}}}, \tag{11}$$

which yields a purely diffusional time dependence of the form

$$T_d(x,t) = \frac{-2\alpha_2^{1/2}}{k_2(1-b_{32})\sqrt{\pi t}} \sum_{m=0}^{\infty} e^{-\tau_m/4\tau}\left(\frac{1+b_{32}}{1-b_{32}}\right)^m, \tag{12}$$

$$\tau_m = \left(\frac{x}{\alpha_3^{1/2}} + \frac{(2m-1)l}{\alpha_2^{1/2}}\right)^2.$$

The results obtained in the present work for the quartz samples of Figs. 10 and 11 clearly demonstrate that diffusional processes dominate the observed impulse response profiles, and the contact resistance effects make no major contribution to the observed signals.

The results of the analysis of Eqs. (9)–(12) apply directly to samples in contact with a semi-infinite pyroelectric detector, and give quantitative results only in this experimental situation. In the present work, sample responses are described quantitatively by the four-layer theory of Part I, incorporating the effects of the detector backing. However, the earlier semi-infinite diffusional theory[6] also applies approximately in the present case, so that the expected time-delay regimes of thermal resistance contributions may be ascertained from Eqs. (9)–(12). The large thicknesses of the quartz samples studied in this work and their associated longer time delays probably explain the absence of obvious contact resistance effects in the experimental time-delay $[h(\tau)]$ profiles recorded in Figs. 10 and 11.

The present results may be contrasted with the work of Sugitani *et al.*,[30] which reported a series of correlation photoacoustic experiments apparently showing the effects of significant contact resistance between sample and backing materials. The contribution of contact resistance was ascertained from the deviation of the time delay versus sample thickness data from the prediction of a model based purely on diffusion. The range of sample thicknesses used in that work was grouped towards a lower range of time delays so that susceptibility to these effects was greater. However, a gas-microphone cell was used as the detection system. Such systems have been known to contribute extraneous time delays to time domain photoacoustic signals due to variations in the flatness of the transducer frequency response[31] and to nonlinearities in response.[32] In the present work, the response of the pyroelectric element is sufficiently fast to permit the observation of thermal signal transit through very thin films. Figure 8 makes a comparison between the response of the PVDF detector element and a 400-μm quartz sample. The frequency response of the detector element is quite flat over the range of signal frequencies corresponding to thermal transit through the material. It is sufficient to note that the rise time of the PVDF detector in our experiments is less than 50 μs, which in much less than the range of responses of the sample reported here.

The results of this work clearly indicate the succcess of the FM-TDS excitation strategy in generating sample responses which agree with the impulse equivalent. The time-delay resolution of our present system is limited, in principle, by the modulation bandwidth of the frequency sweep used for sample excitation. The maximum modulation bandwidth (zero baseband) which is available from our system is 100 kHz, which gives our apparatus a minimum pulse width of less than 10 μs. The early time resolution of the pulsed spectrometer system used by Yeack *et al.*[6] in earlier work was generally poor, with available pulse widths of approximately 1 ms. Departures from the idealized Gaussian pulse shape were suspected as the cause of the early time-scale discrepancies between theory and experiment observed in that work. The pulse shapes available from our system, by contrast, show equivalence to a Dirac delta function, to within the modulation bandwidth of the sweep, without tailing of the excitation/time profile.

These results also compare favorably with earlier broadband photopyroelectric work reported by Coufal.[13] In that work, thin polymer matrices were excited with ac square waves and with random noise modulation. The power spectra of the ac square waves were too narrow to yield a wide dynamic range. Random noise modulation gave excellent power spectral flatness, as expected, with a greatly extended dynamic range. No impulse response information was reported in that work, however. Because random noise excitation strategies are similar to FM-TDS excitation, a detailed comparison has been made between the two methods in Part III of this work.

[1] A. C. Tam and H. Coufal, Appl. Phys. Lett. **42**, 33 (1983).
[2] H. Coufal, IEEE Trans. UFFC, **UFFC-33**, 507 (1986).
[3] A. Mandelis, Chem. Phys. Lett. **108**, 388 (1984).
[4] A. Mandelis and M. M. Zver, J. Appl. Phys. **57**, 4421 (1985).
[5] H. Coufal and P. Hefferle, Can. J. Phys. **64**, 1200 (1986).
[6] C. E. Yeack, R. L. Melcher, and S. S. Jha, J. Appl. Phys. **53**, 3947 (1982).
[7] P. K. John, L. C. M. Miranda, and A. C. Rastogi, Phys. Rev. B **34**, 4342 (1986).
[8] A. Rosencwaig, in *Photoacoustics and Photoacoustic Spectroscopy* (Wiley, New York, 1980), Chap. 2.
[9] W. B. Jackson, N. M. Amer, A. C. Boccara, and D. Fournier, Appl. Opt. **20**, 1333 (1981).
[10] A. Mandelis, Rev. Sci. Instrum. **57**, 617 (1986).
[11] A. Mandelis, L. M. L. Borm, and J. Tiessinga, Rev. Sci. Instrum. **57**, 622 (1986).
[12] A. Mandelis, L. M. L. Borm, and J. Tiessinga, Rev. Sci. Instrum. **57**, 630 (1986).
[13] H. Coufal, J. Photoacoust. **1**, 413 (1984).
[14] J. Opsal and A. Rosencwaig, J. Appl. Phys. **53**, 4240 (1982).
[15] L. C. Aamodt and J. C. Murphy, J. Appl. Phys. **52**, 4903 (1981).
[16] R. M. Miller and G. F. Kirkbright, Anal. Chem. **55**, 502 (1983).
[17] J. S. Bendat and A. G. Piersol, in *Engineering Applications of Correlation and Spectral Analysis* (Wiley, New York, 1980).

[18]A. Mandelis, IEEE Trans. UFFC, **UFFC-33** 590 (1986).
[19]Y. Sugitani, A. Uejima, and K. Kato, J. Photoacoust. **1**, 217 (1982).
[20]R. C. Heyser, J. Audio Eng. Soc. **15**, 370 (1967).
[21]H. Biering and O. Z. Pedersen, Brüel Kjaer Technol. Rev. **1**, 5 (1983).
[22]H. Biering and O. Z. Pedersen, Brüel Kjaer Technol. Rev. **2**, 28 (1983).
[23]KYNAR™ Piezo Film Applications Manual, Pennwalt Corp., King of Purssia, PA, 1983.
[24]Hewlett–Packard model 3562A Dynamic Signal Analyzer Operating Manual, Hewlett Packard, Everett, WA, 1985, pp. 1–20.
[25]J. F. Power and A. Mandelis, Rev. Sci. Instrum. **58**, 2033 (1987).
[26]M. E. Lines and A. M. Glass, *Principles and Applications of Ferroelectrics* (Clarendon, Oxford, 1977).
[27]J. F. Power and A. Mandelis, Rev. Sci. Instrum. **58**, 2018 (1987).
[28]C. R. C. Handbook of Chemistry and Physics, Chemical Rubber Company, Cleveland, OH, 1964.
[29]F. P. Incropera and D. P. DeWitt, *Introduction to Heat Transfer* (Wiley, New York, 1985), Appendix A, pp. 667–696.
[30]A. Uejima, D. Curtis, and Y. Sugitani, J. Photoacoust. **1**, 397 (1983).
[31]A. Mandelis and B. S. H. Royce, J. Appl. Phys. **51**, 610 (1980).
[32]A. Mandelis and J. T. Dodgson, J. Phys. C. **19**, 2329 (1986).